IMAGING RADAR INVESTIGATIONS OF THE SUDBURY STRUCTURE. P. D. Lowman[1], V. H. Singhroy[2], and V. R. Slaney[2], [1]Goddard Space Flight Center, Code 921, Greenbelt MD 20771, USA, [2]Canada Centre for Remote Sensing, 1547 Merivale Road, Ottawa, Ontario K1A 0Y7, Canada.

This paper reports preliminary results of airborne imaging radar studies of the Sudbury structure carried out in preparation for a CCRS European Remote Sensing Satellite (ERS-1) investigation. The data used were synthetic aperture radar (SAR) C-band (5.66 cm) images acquired from about 6 km altitude in 1987. They cover the Sudbury area in both wide and narrow swath modes, with east-west flight paths and north-south illumination directions. Narrow swath resolution is 6 m in range and azimuth; wide swath resolution is 20 m in range and 10 m in azimuth.

The SAR imagery has proven highly effective for field use, providing excellent rendition of topography and topographically expressed structure. Reasons for this include the illumination geometry, notably the look azimuth normal to the long axis of the Sudbury structure and Penokean fold axes, the good spatial resolution, and the short wavelength. Forested areas in the Sudbury area tend to be uniformly rough at C-band wavelength, with backscatter dominated by local incidence angle (i.e., topography). Dielectric properties have relatively little effect on backscatter, except for targets such as metal or water.

Field work using the SAR imagery has to date been concentrated in the North Range and Superior Province as far north as the Benny greenstone belt. This area was chosen for initial investigation of the original size and shape of the Sudbury structure because the effects of the Penokean Orogeny were minimal there. Field work using SAR indicates that there has been little postimpact deformation of the North Range or adjacent Superior Province rock [1]. There appears to be no evidence for an outer ring concentric with the North Range as indicated by early Landsat imagery [2,3]. The apparent ring shown by Landsat is visible on the SAR imagery as the intersection of two regional fracture patterns not related to the Sudbury structure [4]. There is no outer ring visible southwest of the structure. This can reasonably be explained by Penokean deformation, but there is also no outer ring to the northeast cutting the relatively undeformed Huronian sediments of the Cobalt Embayment. Further study of these problems is planned with ERS-1 imagery.

References: [1] Lowman P. D. Jr. (1991) *Can. J. Remote Sens., 17*, 152–161. [2] Dressler B. O. (1984) In *The Geology and Ore Deposits of the Sudbury Structure* (E. G. Pye et al., eds.), Ontario Geological Survey. [3] Grieve R. A. F. et al. (1991) *JGR, 96*, 753–764. [4] Lowman P. D. Jr. (1992) *Rev. Geophys.*, in press.

PHASE TRANSFORMATIONS IN 40–60-GPa SHOCKED GNEISSES FROM THE HAUGHTON CRATER (CANADA): AN ANALYTICAL TRANSMISSION ELECTRON MICROSCOPE (ATEM) STUDY. I. Martinez, F. Guyot, and U. Schärer, Université Paris7 et IPG Paris, 2 place Jussieu, 75251 Paris cedex 05, France.

In order to better understand phase transformations, chemical migration, and isotopic disequilibrium in highly shocked rocks [1], we have performed a microprobe and an ATEM study on gneisses shocked up to 60 GPa from the Haughton Crater.

The Haughton impact structure, Devon Island, is a crater of 24 km in diameter formed in a target of about 1700 m of sedimentary rocks (limestones and dolomites) on top of a crystalline Precambrian gneiss. Samples were all crystalline fragments from the allochthonous polymict breccia [2], which cover the central area of the crater. Optical microscopy on thin sections does not allow identification of minerals by classical criteria: Birefringence of most of the phases (actually all but sillimanite) is largely lost, documenting their essentially amorphous character. Nevertheless, conservation of primary foliation suggests that total rock melting did not occur. These crystalline fragments also show large degrees of porosity, lying roughly at 40%. Electron microprobe analyses reveal five compositional domains: (1) numerous SiO_2 dominant zones, (2) areas with a biotitelike composition, (3) layers with feldsparlike composition, (4) areas characterized by Al/Si close to 1, and (5) fracturated sillimanites.

Strong chemical heterogeneities were observed within most of the compositional domains. To decipher the origin of such heterogeneities, an ATEM study was performed, yielding a spatial resolution of 0.5 nm in image mode and of 200 nm for the energy dispersive X-ray microanalyses (EDS). This study reveals the following chemical and structural characteristics:

1. SiO_2 dominant areas are formed by a mixture of pure SiO_2 polycrystalline quartz identified by electron diffraction pattern and chemical analysis (Fig. 1a) and a silica-rich amorphous phase containing minor amounts of aluminium, potassium, and iron (Fig. 1b).

2. Areas with biotitelike composition are formed by <200-nm grains of iron-rich spinels (Fig. 2a) embedded in a silica-rich amorphous phase (Fig. 2b) that is very similar to the one described above.

3. Layers with feldsparlike composition are constituted by 100–200-nm-sized alumina-rich grains (the indexation of the crystalline structure is under progress) and the silica-rich amorphous phase.

4. Zones characterized by the unusual Al/Si ratio close to 1 are formed by spinel grains (200-nm-sized) embedded in the same silica-rich amorphous phase.

5. The fracturated sillimanites contain domains with a lamellar structure, defined by the intercalation of 100-nm-wide lamellae of mullite crystals and of a silica-rich amorphous phase (Fig. 3a). Figure 3b shows an individual 500-nm-sized crystal of mullite. These crystals preserved the crystallographical orientation of the preshock sillimanite.

All compositional domains, identified at the microprobe scale, can thus be explained by a mixture in different proportion between the following phases: (1) a silica-rich amorphous phase, with minor Al and K; (2) quartz crystals; (3) spinel crystals and alumina-rich crystals; (4) sillimanite; and (5) mullite. Such mixtures of amorphous phases and crystals in different proportions explain disturbed isotope systems in these rocks and chemical heterogeneities observed on the microprobe.

References: [1] Schärer U. and Deutsch A. (1990) *GCA, 54*, 3435–3447. [2] Metzler A. et al. (1988) *Meteoritics, 23*, 197–207.

PHASE TRANSFORMATIONS IN 40–60-GPa SHOCKED GNEISSES FROM THE HAUGHTON CRATER (CANADA):
Martinez I. et al.

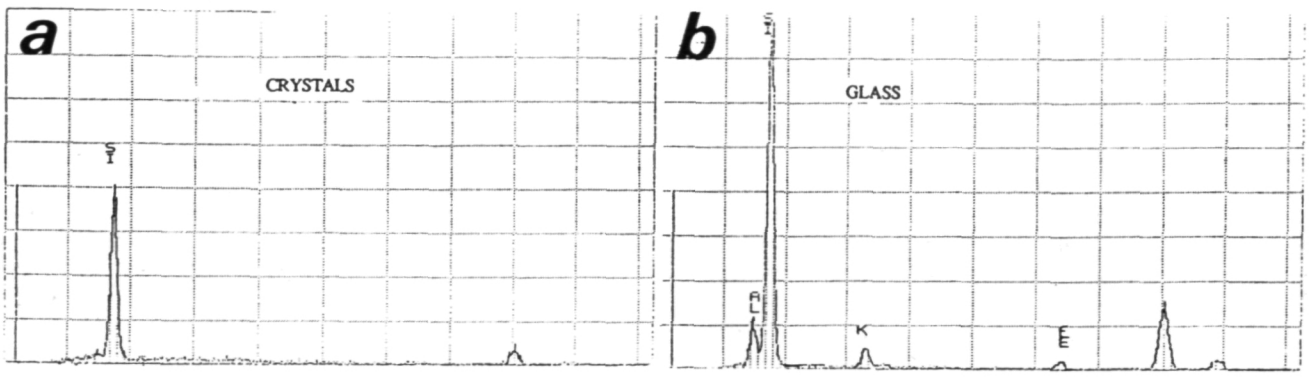

Fig. 1. **(a)** EDS microanalysis of polycrystalline quartz. Oxygen is not detectable with this EDS configuration and some contamination by the copper of the sample support occurs; **(b)** EDS microanalysis of the silica-rich amorphous phase.

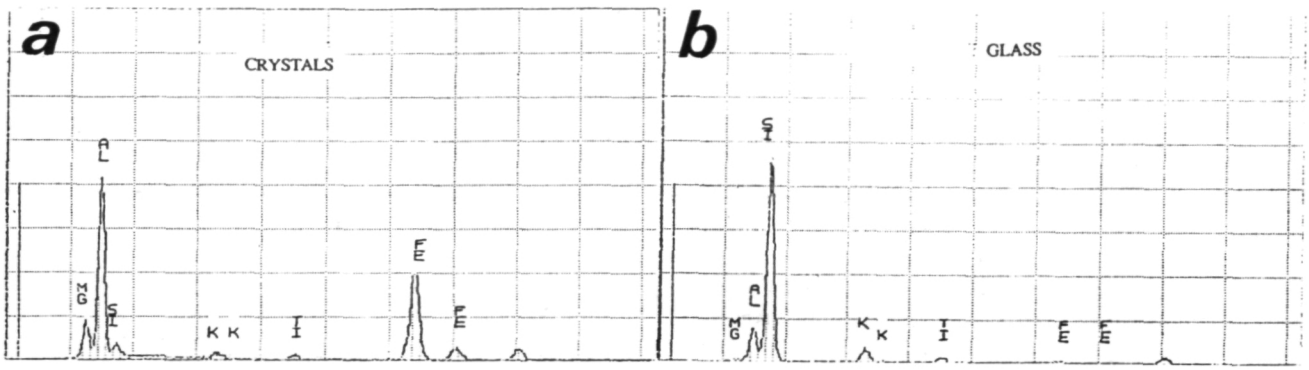

Fig. 2. **(a)** EDS microanalysis of an iron-rich spinel crystal. The composition is approximately $(Mg_{0.5}Fe_{0.5})Al_2O_4$, although Fe^{3+} could not be determined; **(b)** EDS microanalysis of the silica-rich amorphous phase. Notice the similarity with Fig. 1b.

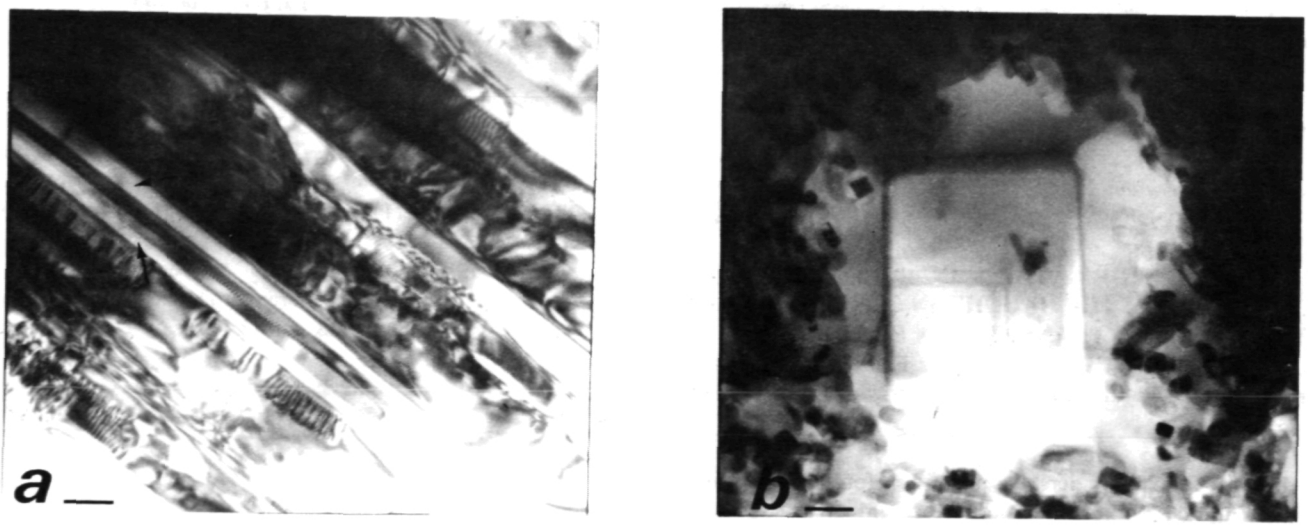

Fig. 3. **(a)** TEM image of the lamellar structure of intercalated mullite and silica-rich (+Al,K) amorphous phase (see arrows). Scale bar is 200 nm. **(b)** In some areas, mullite appears as small euhedral crystals surrounded by the amorphous phase. TEM, scale bar 200 nm.